

# Multiple-Period Adaptive-Repetitive Control of a Hard Disk Drive

Néstor O. Pérez-Arancibia, Tsu-Chin Tsao and James S. Gibson

**Abstract**—This paper introduces a new method for synthesizing multiple-period repetitive controllers, which are suitable for integration into a combined adaptive-repetitive control scheme. The proposed synthesis method can be implemented recursively reducing the complexity of controller design considerably when compared with other methods available in the literature. In order to exemplify the synthesis procedure, a multiple-period adaptive-repetitive controller is designed for track-following control of a commercial hard disk drive and implemented in real-time using a digital signal processor. Experimental results show the effectiveness of the approach introduced in this work.

## I. INTRODUCTION

Repetitive control [1], [2] has been demonstrated to be very effective in rejecting disturbances when implemented on systems affected by periodic disturbances, such as, *hard disk drives* (HDD), electric motors and generators, other rotating machines, and satellites. Also, repetitive control has been shown to be an appropriate tool when applied to periodic tracking problems in power electronics, manufacturing and robotics. In both kind of problems, disturbance rejection and tracking, it is not rare to encounter applications where controllers capable of dealing with signals composed of multiple periods are required. Common examples are electromechanical systems containing multiple gears. This paper is devoted to the development of a new method for synthesizing repetitive controllers capable of rejecting multi-periodic output disturbances affecting the plant to be controlled.

The main feature of the method introduced here is that it produces multiple-period controllers suitable for integration into the combined adaptive-repetitive control scheme presented in [3], which is based on the notions of *internal model* [4] and *adaptive minimum-variance regulation* [5]. The first part of this paper deals with the reformulation of the original disturbance rejection control problem as a polynomial algebraic one, and also, with finding an explicit analytical solution for it. In general, the existence of a solution with an explicit analytical expression does not guarantee simple computability. For this reason, the second part of this paper presents the development of a recursive algorithm that reduces significantly the complexity of control synthesis.

Previous works have addressed the problem of multiple-period repetitive control, from both theoretical and practical

perspectives, e.g., [6], [7], [8]. However, those solutions are not easily integrable into the scheme presented in [3], considered here. For that reason, in this work we introduce an alternative approach, which extends the methods for designing one-period adaptive-repetitive controllers in [3] to the multi-periodic case, following the ideas and guidelines in [9], [10], [2] and [11]. Experimental results obtained using a commercial HDD demonstrate the effectiveness of the resulting control synthesis method.

The rest of the paper is organized as follows. Section II reviews some fundamentals concepts of repetitive control. Section III presents the main contribution of this paper, which is a new method for synthesizing multiple-period repetitive controllers. Section IV describes a multiple-period adaptive-repetitive control scheme. Section V presents experimental results. Finally, some conclusions are given in Section VI.

## II. PRELIMINARIES ON REPETITIVE CONTROL

### A. One-Period Repetitive Control for Disturbance Rejection

In this section, we review some fundamental ideas on one-period repetitive control that will be used later in this paper. First, consider the block diagram in Fig. 1. There,  $G$  is a stable *linear time-invariant* (LTI) system and  $w$  is a disturbance considered to be mostly formed by a combination of sinusoidal sequences with frequencies multiple of a fundamental one. If the original plant system is unstable, it is assumed that it can be stabilized by LTI feedback control.



Fig. 1. LTI plant  $G$  and output disturbance  $w$ .

To begin with, we describe a repetitive control method for feedforward disturbance rejection in which the signal  $w$  is assumed to be available for measurement. This is a design assumption, since in practice  $w$  can be estimated but not directly measured. Also, it is assumed that the fundamental frequencies of the periodic signals forming part of  $w$  are a priori known. Thus, the natural control goal is the synthesis of a stable feedforward filter  $K$ , such that, the frequency response of the LTI system  $1 - KG$  is zero, or close to zero, at the same periodic frequencies of the sinusoidal signals composing  $w$ . This approach results in the block diagram in Fig. 2, where

$$y = w - GKw = (1 - GK)w. \quad (1)$$

This work was supported by the NSF Center for Scalable and Integrated Nanomanufacturing under Grant DMI-0327077 and Grant CMMI-0327077, and by the Office of Naval Research under Grant N00014-07-1-1063.

The authors are with the Mechanical and Aerospace Engineering Department, University of California, Los Angeles, CA, 90095-1597, USA. nestor@seas.ucla.edu, ttsao@seas.ucla.edu, gibson@ucla.edu.

Notice that the problem posed as in Fig. 2 becomes a feedforward tracking control problem. It is immediately clear that for the ideal case where  $G$  is minimum phase with relative degree 0, the best choice is to pick  $K = G^{-1}$ . However, it is not unusual to encounter discrete-time systems, obtained from sample-and-hold equivalence of continuous-time systems, that have unstable zeros. An alternative approach, the one chosen here as in [3], is to define an error transfer function  $E = 1 - GK$  and then force the frequency response of  $E$  to be zero periodically at certain desired frequencies. This objective is achievable by using the polynomial design methods in [9], following the general guidelines presented in [2] and [10]. The main idea is to enforce an error transfer function with the form  $E = RD$ , where  $D$  can be thought of as an internal model for the disturbance  $w$  and  $R$  is an a priori unknown stable transfer function. For the one-periodic class of signals considered in this section, the internal model is chosen to be

$$D = 1 - qz^{-N}, \quad (2)$$

where  $q$  is a zero-phase low-pass filter and  $N$  is the period of the periodic disturbance to be attenuated.

The filter  $q$  will allow us some flexibility over the frequency range of disturbances to be canceled while maintaining stability. The filter  $D$  has a combed shape with notches matching the frequencies of the periodic signals forming part of  $w$ . Thus, a filter  $K$  that makes the frequency response of  $E$  close to zero at desired periodic frequencies can be computed by solving the Diophantine equation

$$RD + KG = 1, \quad (3)$$

where  $R$  and  $K$  are the unknowns. Similar approaches but with slightly different internal models can be found in [12] and references therein.

Now, we briefly discuss the existence of solutions for (3). First, notice that (3) can be rearranged as

$$b_R(a_K a_G b_D) + b_K(a_R a_D b_G) = a_K a_G a_R a_D, \quad (4)$$

where the polynomial numerators are denoted by the symbol  $b$ , the polynomial denominators by the symbol  $a$  and the subindices indicate the corresponding transfer function in (3). It is immediate from [9], and references therein, e.g., [13], that for given polynomials  $a_G$ ,  $b_D$ ,  $a_D$  and  $b_G$  and chosen polynomials  $a_K$  and  $a_R$ , (4) has a solution if and only if the greatest common factor of  $a_K a_G b_D$  and  $a_R a_D b_G$  divides  $a_K a_G a_R a_D$ . In general if this condition is satisfied, we say that  $G$  and  $D$  are coprime.

As shown in [2] if a solution pair  $\{R_o, K_o\}$  is found, then (3) characterizes a whole family of stabilizing internal

model-based repetitive controllers. As in [3], following the guidelines in [2] and [10], a method for finding a particular solution pair  $\{R_o, K_o\}$  is presented here. The method starts by separating  $G$  into its minimum and non-minimum phase parts, denoted by  $G_+$  and  $G_-$  respectively. Thus,

$$G = \frac{B}{A} = \frac{B_+ B_-}{A} = G_+ G_-, \quad (5)$$

$$G_+ = \frac{B_+}{A}, \quad G_- = B_-.$$

Where all the zeros of  $B_+$  are stable, and all the zeros of  $B_-$  are unstable. Often,  $B_+$  and  $B_-$  are referred as the cancelable and uncancelable parts of the numerator  $B$  of  $G$ , respectively. Now, substituting (5) into (3) we can write

$$RD + \kappa G_- = 1, \quad \kappa = KG_+. \quad (6)$$

Among the infinity many solutions to (6), it is verifiable by simple algebraic manipulations that one of the solutions is given by

$$R_o = \frac{1}{1 - (1 - \gamma G_-^* G_-) q z^{-N}}, \quad (7)$$

$$\kappa_o = q \gamma G_-^* z^{-N} R_o, \quad K_o = \kappa_o G_+^{-1}.$$

Here,  $G_-^*$  is defined as  $G_-^*(z^{-1}) = G_-(z)$ , and  $0 < \gamma \in \mathbb{R}$ . From this point onwards, in block diagrams and equations we employ the symbols  $K_o$  and  $R_o$ , under the understanding that those correspond to the specific solution in (7).

The block diagram in Fig. 2 assumes that the signal disturbance  $w$  is available for measurement. However, in practice  $w$  has to be estimated on-line according the diagram in Fig. 3, where  $\hat{G}$  is an identified model of  $G$  and  $\hat{w}$  is the estimate of  $w$ . Clearly, when the estimation scheme shown in Fig. 3 is employed, the feedforward disturbance cancelation filter  $K_o$  becomes part of a feedback controller  $v_o$  computable as

$$v_o = \frac{-K_o}{1 - K_o \hat{G}}. \quad (8)$$

It is immediately noticeable that the stability and performance of the closed-loop system, resulting from the interconnection of  $G$  and the *single-input-single-output* (SISO) LTI controller  $v_o$ , can be analyzed using all the tools of classical control, such as, gain and phase margins, along with the use of sensitivity functions. In this case, we are interested in the output disturbance sensitivity function

$$\zeta_o = \frac{1}{1 - G v_o}. \quad (9)$$

Notice that under the assumption that  $\hat{G} = G$ , it follows that

$$\zeta_o = 1 - G K_o, \quad (10)$$

which is the feedforward mapping from  $w$  to  $y$ , shown in Fig. 2. This implies that the closed-loop performance is not altered by the estimation process as long as the model  $\hat{G}$  is an exact representation of the true plant  $G$ .

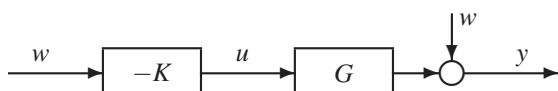


Fig. 2. Feedforward output disturbance rejection scheme.

The previous development establishes that the closed-loop system will be stable for stable plants  $G$  and  $K_o$ , under the assumption that  $\hat{G} = G$ . Thus, we need a method to ensure that the design algorithm produces a stable  $K_o$ . This is discussed in the next subsection.

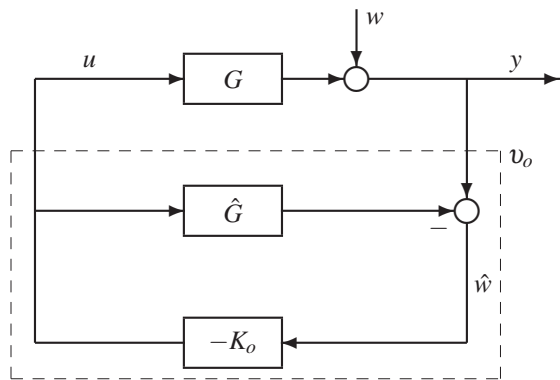


Fig. 3. Estimation of  $w$  and repetitive control scheme.

### B. Nominal Stability Analysis

In order to have a nominally stable closed-loop system all what needs to be done is to ensure that the design algorithm yields a stable controller  $K_o$ . Recalling the definition of  $K_o$  in (7), notice that  $K_o$  is formed by the multiplication of the systems  $q\gamma G_-^* z^{-N}$ ,  $R_o$ , and  $G_+^{-1}$ . By definition  $G_+^{-1}$  is stable. The system  $q\gamma G_-^* z^{-N}$  is stable and causal provided that  $q$  is stable and that  $N$  is large enough. Thus,  $K_o$  will be stable as long as  $R_o$  is stable. Here, we state a sufficient condition for the stability of  $R_o$  which is based on the *small gain theorem* [14]. First, notice that  $R_o$  can be represented by the block diagram in Fig. 4, where  $N = N_a + N_b$ , such that,  $z^{-N_a}$  and  $z^{-N_b}$  make the systems  $qz^{-N_a}$  and  $(1 - \gamma G_-^* G_-) z^{-N_b}$  causal, respectively.

The small gain theorem implies that a sufficient condition for asymptotic stability is

$$\|(1 - \gamma G_-^* G_-) z^{-N_b}\|_\infty \|qz^{-N_a}\|_\infty < 1, \quad (11)$$

which can be translated into

$$|1 - \gamma G_-^*(e^{j\theta}) G_-(e^{j\theta})| < \frac{1}{|q(e^{j\theta})|}, \quad \forall \theta \in [0, \pi]. \quad (12)$$

In (12) the real number  $\gamma$  can be thought of as a stability and performance tuning parameter. It is important to emphasize that when (12) is satisfied, the resulting controller  $K_o$  is stable and consequently the closed-loop system is stable as well. The systems involved are LTI, therefore, an appropriate way to analyze stability robustness is the use of the notions of gain and phase margins, from classical control theory. This approach will be employed in the design examples to be presented later in this paper.

## III. MULTIPLE-PERIOD REPETITIVE CONTROL

### A. Proposed Controller Design Method

In this subsection we introduce the main contribution of this paper, which is a new method for synthesizing

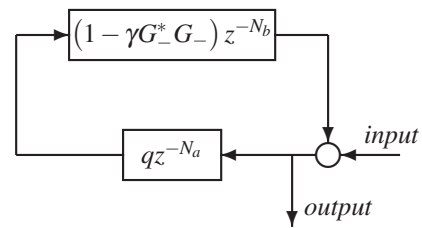


Fig. 4. Representation of  $R_o$  as a typical feedback configuration.

multiple-period repetitive controllers. The design method for synthesizing one-period repetitive controllers presented in the previous section can be integrated into a combined adaptive-repetitive controller scheme to be presented in Section IV. In order to design a multiple-period adaptive-repetitive controller with the same capability, we need to solve (6) with a corresponding multiple-period internal model  $D$ . From the internal model principle, it follows that for targeting  $L$  different periods a suitable  $L$ -period  $D$  is given by

$$D = \prod_{k=1}^L 1 - q_k z^{-N_k}. \quad (13)$$

Thus, the next step is to solve (6) with the internal model in (13). In order to accomplish that, first we need to define some concepts to be used later.

**Definition 1.** An  $r$ -combination of a set is a subset of size  $r$ . For example, for the set  $\{a, b, c\}$ , we have the following three 2-combinations:  $\{a, b\}$ ,  $\{a, c\}$  and  $\{b, c\}$ .

**Definition 2.** For a LTI system  $G_-$ , exponentials are defined as follows:  $G_-^0 = 1$  and  $G_-^k = G_- G_- \dots G_-$ ,  $k$  times.

**Definition 3.** For a number  $k \in \mathbb{N}$  (being  $\mathbb{N}$  the set of natural numbers), the system  $f_k$  is defined as

$$f_k = \frac{G_-^* q_k \gamma_k z^{-N_k}}{1 - (1 - \gamma_k G_-^* G_-) q_k z^{-N_k}}, \quad (14)$$

where  $q_k$  is a zero-phase low-pass filter,  $0 < \gamma_k \in \mathbb{R}$  (being  $\mathbb{R}$  the set of real numbers), and  $N_k \in \mathbb{N}$ .

With the use of the previous definitions we state a theorem that will serve as a guideline for synthesizing multiple-period repetitive controllers.

**Theorem 1.** A particular solution to the  $L$ -period problem is given by

$$R_o = \prod_{k=1}^L \frac{1}{1 - (1 - \gamma_k G_-^* G_-) q_k z^{-N_k}}, \quad (15)$$

and by

$$\kappa_o = \sum_{k=1}^L \sum_{s \in S_k} (-1)^{k+1} G_-^{k-1} F_{ks}, \quad K_o = \kappa_o G_+^{-1}, \quad (16)$$

with

$$F_{ks} = \prod_{j=1}^k f_{s_j}, \quad (17)$$

where  $s$  is a vectorial index  $s = \{s_1, \dots, s_k\} \in \mathbb{N}^k$  and  $S_k$  is the set that contains all the  $k$ -combinations of the set

$\{1, 2, \dots, k, \dots, L\}$ . The functions  $f_{s_j}$  are computed according to (14).

**Proof.** Notice that relation (16) holds if and only if the system  $\kappa_o^{(n+1)}$  for the  $(n+1)$ -period case can be computed recursively from the system  $\kappa_o^{(n)}$  for the  $n$ -period case as

$$\kappa_o^{(n+1)} = \kappa_o^{(n)} - \kappa_o^{(n)} G_- f_{n+1} + f_{n+1}, \quad (18)$$

with  $\kappa_o^{(1)}$  given by (7). Notice that the superscripts in parentheses,  $(n+1)$ ,  $(n)$ , etc. refer to the recursion number and they do not denote exponentials as in Definition 2.

Also, it is immediate that

$$R_o^{(n+1)} = \frac{R_o^{(n)}}{1 - (1 - \gamma_{n+1} G_-^* G_-) q_{n+1} z^{-N_{n+1}}}, \quad (19)$$

with  $R_o^{(1)}$  given by (7). Thus, having the solution given by (18) and (19) a recursive form, it is proven using mathematical induction.

- For  $n = 1$ : It follows immediately from (7).
- For  $n + 1$  assuming the solution for  $n$ : What needs to be shown is that relations (18) and (19) satisfy

$$R_o^{(n+1)} D^{(n+1)} + \kappa_o^{(n+1)} G_- = 1, \quad (20)$$

provided that

$$R_o^{(n)} D^{(n)} + \kappa_o^{(n)} G_- = 1. \quad (21)$$

To show that (18), (19) and (21) imply (20), the right side of (18) and the right side of (19) are replaced into the left side of (20). Thus, we obtain

$$\frac{\frac{R_o^{(n)} D^{(n)} + \kappa_o^{(n)} G_-}{1 - (1 - \gamma_{n+1} G_-^* G_-) q_{n+1} z^{-N_{n+1}}} - (R_o^{(n)} D^{(n)} + \kappa_o^{(n)} G_-) q_{n+1} z^{-N_{n+1}} - \gamma_{n+1} G_-^* G_- q_{n+1} z^{-N_{n+1}}}{1 - (1 - \gamma_{n+1} G_-^* G_-) q_{n+1} z^{-N_{n+1}}}.$$

Now, noticing (21), it follows that the numerator and denominator in (22) are identical, then (20) follows, and therefore, (15) and (16) follow as well, which completes the proof of Theorem 1. ■

**Remark 1.** Notice that the previous proof is constructive, and therefore, (18) gives us a recursive method for synthesizing controllers for an arbitrary number of periods.

**Remark 2.** One could naively think that an internal model with the form of (13) is not necessary and that it would be enough to consider an internal model with the form of (2), with  $N$  being the least common multiple of all the  $N_k$ ,  $k = 1, \dots, L$ . However, this would produce sensitivity functions with an unnecessarily large number of notches, and also this could lead to numerically untractable problems. For example, consider the case  $N_1 = 3$ ,  $N_2 = 4$ , with  $L = 2$ . In this case if we were to solve the problem using an internal model with the form of (2), the  $N$  corresponding to the least common multiple of  $N_1 = 3$  and  $N_2 = 4$  would be 12, which implies that the resulting sensitivity function would have 12 notches

on the range  $[0, f_s]$ , where  $f_s$  is the sampling frequency. On the other hand, if we were to solve the same problem using an internal model with the form of (13), the resulting sensitivity function would have 7 notches on the range  $[0, f_s]$ , only.

A more dramatic case is  $N_1 = 78$ ,  $N_2 = 134$ , with  $L = 2$ , to be considered in the experimental section. In this case,  $N_1 + N_2 = 212$ , whereas the least common multiple of  $N_1 = 78$  and  $N_2 = 134$  is 5,226!

In the following paragraphs we show examples aimed to explain the proposed controller synthesizing process.

**Example 1.** Consider a generic case with  $L = 3$ . The computation of  $R_o^{(3)}$  follows from (15). The computation of  $\kappa_o^{(3)}$  is done as follows.

To begin with, we compute the systems defined by (17). For  $k = 3$ , the only 3-combination of the set  $\{1, 2, 3\}$  is  $\{1, 2, 3\}$ , then  $S_3 = \{\{1, 2, 3\}\}$ , and therefore, we have

$$F_{3\{1,2,3\}} = f_1 f_2 f_3.$$

For  $k = 2$ , the 2-combinations of the set  $\{1, 2, 3\}$  are  $\{1, 2\}$ ,  $\{1, 3\}$  and  $\{2, 3\}$ , then  $S_2 = \{\{1, 2\}; \{1, 3\}; \{2, 3\}\}$ , and therefore, we have

$$F_{2\{1,2\}} = f_1 f_2; \quad F_{2\{1,3\}} = f_1 f_3; \quad F_{2\{2,3\}} = f_2 f_3.$$

For  $k = 1$ , the 1-combinations of the set  $\{1, 2, 3\}$  are  $\{1\}$ ,  $\{2\}$  and  $\{3\}$ , then  $S_1 = \{\{1\}; \{2\}; \{3\}\}$ , and therefore, we have

$$F_{1\{1\}} = f_1; \quad F_{1\{2\}} = f_2; \quad F_{1\{3\}} = f_3.$$

Now, we compute the interior sums in (16). For  $k = 3$ , the interior sum is

$$\sum_{s \in S_3} F_{3s} = f_1 f_2 f_3.$$

For  $k = 2$ , the interior sum is

$$\sum_{s \in S_2} F_{2s} = f_1 f_2 + f_1 f_3 + f_2 f_3.$$

For  $k = 1$ , the interior sum is

$$\sum_{s \in S_1} F_{1s} = f_1 + f_2 + f_3.$$

Thus,  $\kappa_o^{(3)}$  is given by

$$\kappa_o^{(3)} = f_1 + f_2 + f_3 - G_- (f_1 f_2 + f_1 f_3 + f_2 f_3) + G_-^2 f_1 f_2 f_3.$$

**Remark 3.** Notice that given that the vectorial indices  $s$  are formed using the concept of  $r$ -combination, the order of the elements in  $s$  is irrelevant, and therefore, permutations of the elements in  $s$  do not change the index. For example, consider  $S_2$  in Example 1. There, if the second index in  $S_2$ ,  $\{1, 3\}$ , is replaced by  $\{3, 1\}$ , the result remains invariant since  $F_{2\{3,1\}} = f_3 f_1 = f_1 f_3 = F_{2\{1,3\}}$ .

As stated in Remark 1, relation (18) gives us a method for synthesizing repetitive controllers with any number of periods recursively. This is illustrated with the following example.

**Example 2.** We consider the same problem in Example 1, but we solve it recursively. To begin with, we notice that

$$\kappa_o^{(1)} = f_1.$$

The second recursion is given by

$$\kappa_o^{(2)} = f_1 - f_1 G_- f_2 + f_2.$$

And finally the third recursion solves the problem as

$$\begin{aligned} \kappa_o^{(3)} &= f_1 - f_1 G_- f_2 + f_2 - (f_1 - f_1 G_- f_2 + f_2) G_- f_3 + f_3 \\ &= f_1 + f_2 + f_3 - G_- (f_1 f_2 + f_1 f_3 + f_2 f_3) + G_-^2 f_1 f_2 f_3. \end{aligned}$$

### B. Nominal Stability Analysis

The first thing to notice is that the controller  $K_o$  is formed by summations and products of transfer functions  $f_k$ ,  $k = 1, \dots, L$  with themselves and with the plant  $G_-$ . Therefore, if each transfer function in the set  $\{f_1, f_2, \dots, f_L\}$  is stable, then the resulting controller  $K_o$  will be stable as well. Thus, following the development in the previous section, it is clear that a sufficient condition for stability is

$$\left| 1 - \gamma_k G_-^* (e^{j\theta}) G_- (e^{j\theta}) \right| < \frac{1}{|q_k(e^{j\theta})|}, \quad \forall \theta \in [0, \pi] \quad (23)$$

for  $k = 1, \dots, L$ .

This condition might look conservative. However, in the experimental section, we show that it is an appropriate guideline for design.

## IV. AN ADAPTIVE-REPETITIVE CONTROL SCHEME

### A. Repetitive and Minimum-Variance Control

The principal reason for solving the repetitive control problem as in the previous sections is that this method allows us to formulate a  $H_2$  control problem, which can be approximated by the adaptive scheme presented in [3], described here. To begin with, let us consider an arbitrary rational LTI asymptotically stable filter  $Q$ , i.e.,  $Q \in RH_\infty$ . Also, let

$$R(Q) = R_o - QG, \quad (24)$$

$$K(Q) = K_o + QD. \quad (25)$$

It is clear that systems  $R(Q)$  and  $K(Q)$  in (24) and (25) define an entire family of solutions to the Diophantine equation in (3). Notice that  $R(Q)$  and  $K(Q)$  belong to  $RH_\infty$  for all  $Q \in RH_\infty$ , provided that  $D$  and  $G$  are stable.

The previous parametrization allows us to formulate a new control problem as an optimization one. Specifically, we would like to minimize the variance of the system output random variable  $\mathbf{y}(k) \forall k$ . Notice that from this perspective, the sequence  $y$ , in Fig. 2 and other figures, is a realization of the random process  $\mathbf{y}$ . Now, let  $\mathbf{y}$  be a stationary mean-ergodic and covariance-ergodic random process for any given stable LTI filter  $Q$ . Then, the problem becomes

$$\min_{Q \in RH_\infty} E\{\mathbf{y}^2(k)\}. \quad (26)$$

Notice, that if  $E\{\mathbf{y}^2(k)\} = \sigma^2$ , the ergodicity assumption implies that  $\lim_{N \rightarrow \infty} \frac{1}{N} \sum_{k=0}^N y^2(k) = \sigma^2$ , with probability 1. Also, it is verifiable that (26) is equivalent to the  $H_2$  problem

$$\min_{Q \in RH_\infty} \|W - GK(Q)W\|_2, \quad (27)$$

where  $W$  is a stable filter that maps a stationary, white, zero-mean, unit-variance random sequence to the disturbance  $w$ . Filters like  $W$  are usually called disturbance models of  $w$ . Considering (3) and the parameterized systems  $K(Q)$  and  $R(Q)$ , (27) is equivalent to

$$\min_{Q \in RH_\infty} \|R_o DW - QGDW\|_2. \quad (28)$$

It is important to remark that the solution to (27) requires a disturbance model  $W$ . In practice the identification of an accurate model  $W$  is extremely difficult and often impossible, and also, it is not clear how a solution to (27) can be adaptively approximated. Fortunately, (28) can be approximated with the use of adaptive filters. This is key in the development of the adaptive-repetitive control scheme to be introduced later in this section.

### B. Stability of the Closed-loop System with $K(Q)$

Similarly to the case studied in Section II, if the controller  $K_o$  in Fig. 3 is replaced by  $K(Q)$ , then under the assumption that  $\hat{G} = G$ , the sensitivity function from the disturbance  $w$  to the output  $y$  is given by

$$\zeta_{K(Q)} = 1 - GK(Q). \quad (29)$$

This implies that for stable systems  $K_o$ ,  $D$  and  $Q$ , the closed-loop system is nominally stable. Clearly, for any LTI  $Q$ , the stability robustness of the closed-loop system can be analyzed using classical indices, such as, gain and phase margins.

For reasons that will become clear in the next subsection, many times it results useful to look at the stability problem from an alternative perspective. For that purpose, let us consider plant additive uncertainty, i.e.,

$$G = \hat{G} + \Delta_G, \quad (30)$$

and then, replace  $K_o$  by the new controller  $K(Q)$ . Thus, the block diagram in Fig. 3 is equivalent to the block diagram in Fig. 5, which implies that, invoking the *small gain theorem* [14], a sufficient stability condition is given by

$$\|\Delta_G\|_\infty \|K(Q)\|_\infty < 1. \quad (31)$$

It is worth mentioning that this condition is consistent with the feedforward stability condition based on (29), since for the case  $\hat{G} = G$ , the system is always stable.

Thus far, we have assumed that  $Q$  is a stable LTI system, however, it is important to note that for the case in which  $Q$  is time-varying, the condition remains essentially the same, except for the replacement of the  $H_\infty$  norm ( $\|\cdot\|_\infty$ ) by the  $\ell_2$ -induced norm ( $\|\cdot\|_{\ell_2 \rightarrow \ell_2}$ ). This fact will be used in the next subsection.

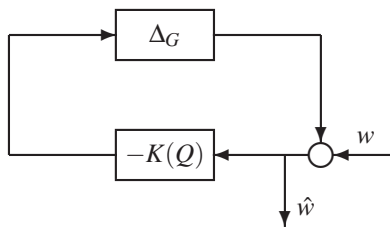


Fig. 5. Systems  $\Delta_G$  and  $K(Q)$  in typical feedback configuration.

### C. Proposed Adaptive Scheme

The solution to (28) can be found employing well-known  $H_2$  control methods [15]. However, in order to apply those methods we would need a reliable model  $W$  capable of capturing all the relevant statistical information contained in the disturbance signal  $w$ . A system  $W$  can be identified using some identification method. For example, in [16] disturbance models are identified using the *n4sid* subspace method.

In most applications the identification of disturbance models is challenging and often times impossible. For this reason, it is convenient to translate the problem in (28) into an adaptive filtering problem, solvable online by the use of algorithms such as RLS (*recursive least-squares*) or LMS (*least-mean-squares*). In this case, the standard LMS algorithm and the inverse QR-RLS algorithm in [17] are employed to demonstrate the proposed method in experiments. The proposed adaptive scheme is shown in Fig. 6, where the controller  $K(Q) = K_o + QD$  can be broken into a repetitive part,  $K_o$ , and an adaptive part,  $QD$ .

The fundamental idea behind the scheme is that the adaptive algorithm is run using a regressor formed by values from the signal  $Dw$ , and not  $w$ , as in the typical minimum-variance adaptive configurations. Thus, the periodic content to be canceled in  $w$  is attenuated by  $K_o$ , and what is left,  $Dw$ , is attenuated adaptively. In the experiments presented in this paper, we introduce the constraint  $Q(z) = \sum_{i=0}^{N_Q} \theta_i z^{-i}$ , where  $N_Q$  is the order of the filter  $Q$  and  $\theta_i \in \mathbb{R}$ . This allows us to enforce the stability of  $Q$ , since *finite impulse response* (FIR) filters are always stable provided that the coefficients remain bounded.

The stability arguments given in the previous section, for the case when  $Q$  is LTI, can be easily extended to the case when  $Q$  is time-varying. Notice that under the assumption that  $\hat{G} = G$ , the system in Fig. 6 will be  $\ell_2$ -stable for any  $\ell_2$ -stable  $Q$ . Similarly to the LTI case, if additive uncertainty is assumed as in (30), the system in Fig. 6 will remain  $\ell_2$ -stable as long as the  $\ell_2$ -induced norm of  $K(Q)$  remains small enough.

## V. EXPERIMENTS

### A. Description of the Experiment

The experimental effectiveness of the proposed control scheme is demonstrated on a commercial HDD system. The description of the HDD system and the details of the experimental implementation are discussed in [16]. Here, we

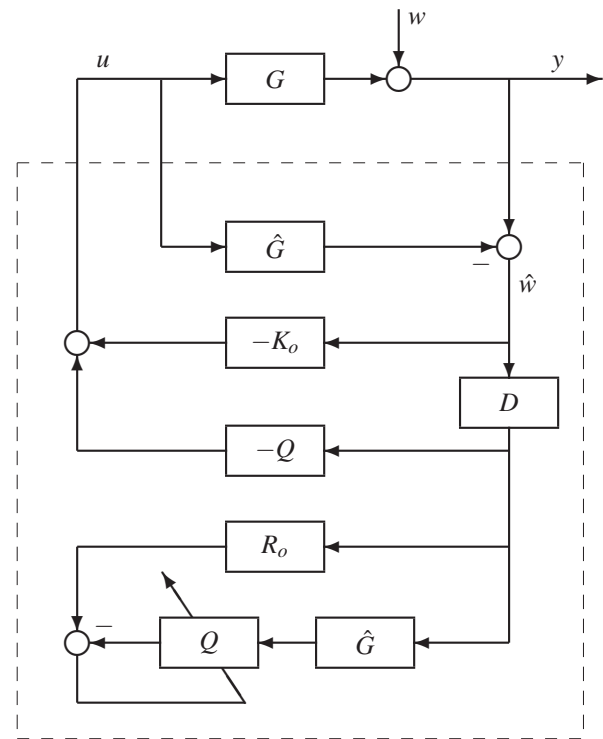


Fig. 6. Adaptive-repetitive control scheme.

focus on track-following, that is, the control objective is to position the center of the HDD head over the center of a HDD data track. As customary, our performance index is the deviation of the center of the head from the center of a given track, often called *track misregistration* (TMR), quantified as

$$TMR = 3\sigma, \quad (32)$$

where  $\sigma$  is the empirical standard deviation of the *position error signal* (PES), expressed as a percentage of the track pitch.

In the experiments presented here, we use a 2-platter (10 GB/platter) 4-head 7,200 rpm commercial HDD and a *Mathworks*<sup>®</sup> xPC Target system for control with a sample-and-hold rate of 9.36 KHz. As a baseline for adding the disturbance rejection scheme discussed here, we use a combination of two LTI control systems, developed and implemented as shown in [16]. These systems are a simple LTI controller and a LTI minimum-variance-type controller, tuned using the inverse QR-RLS algorithm. The closed-loop plant, resulting from the interconnection of those controllers with the original open-loop plant of the HDD system, is  $G$ . A model of  $G$ , labeled as  $\hat{G}$ , was identified using the *n4sid* algorithm. For more details see [3], [16] and [18].

### B. Multiple-Period Repetitive Controller Design

The *power spectral density* (PSD) of the experimental PES  $y$ , obtained using the baseline controller shows that several sets of periodic signals are composing part of the baseline PES  $y$ . Besides the set of signals with frequencies multiple of 120 Hz, which is a direct consequence of the

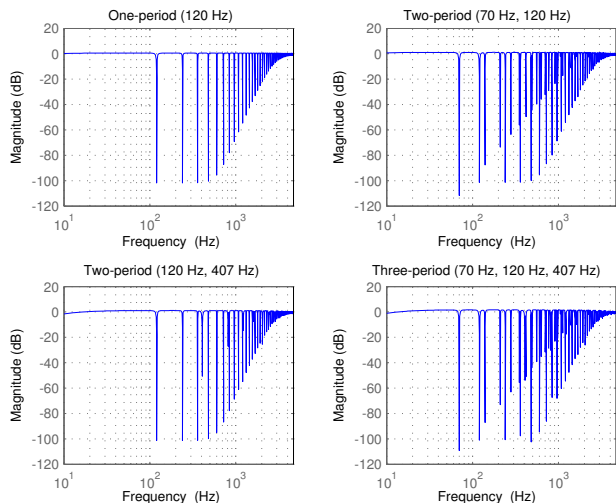


Fig. 7. Sensitivity function  $\zeta_o$  for the cases one-period (120 Hz); two-period (70 Hz, 120 Hz); two-period (120 Hz, 407 Hz); and three-period (70 Hz, 120 Hz, 407 Hz).

rotation of the HDD platters, there are sets of signals with frequencies multiple of 70 Hz, 407 Hz and others. In order to target these periodic signals in the PES, four repetitive controllers are designed, using the methodology described in Section II and Section III. The first controller is one-periodic repetitive aiming to cancel signals with frequencies multiple of 120 Hz. The second controller is two-periodic repetitive aiming to cancel signals with frequencies multiple of 70 Hz and 120 Hz. The third controller is two-periodic repetitive aiming to cancel signals with frequencies multiple of 120 Hz and 407 Hz. And finally, the fourth controller is three-periodic repetitive aiming to cancel signals with frequencies multiple of 70 Hz, 120 Hz and 407 Hz.

In order to generate the notches that would allow us to cancel signals with the aforementioned frequencies, we pick internal models  $D^{(1)}$ ,  $D^{(2)}$  and  $D^{(3)}$  with  $N_1 = 78$ ,  $N_2 = 134$  and  $N_3 = 23$ , respectively. Notice that  $N_1 = 78$  generates notches with an exact period of 120 Hz. However,  $N_2 = 134$  and  $N_3 = 23$  generate notches with periods of 69.8507 Hz and 406.9565 Hz, respectively. The corresponding low-pass zero-phase filters  $q_1$ ,  $q_2$ ,  $q_3$  are given by

$$q_3 = q_2 = q_1 = \left(1 - 10^{-6}\right) \left[2(2q_0 - q_0^2) - (2q_0 - q_0^2)^2\right], \quad (33)$$

with  $q_0(z^{-1}, z) = 0.2z^{-1} + 0.6 + 0.2z$ . The corresponding parameters  $\gamma_1$ ,  $\gamma_2$  and  $\gamma_3$  are given by  $\gamma_3 = \gamma_2 = \gamma_1 = 4.5 \times 10^{-7}$ .

The filters  $q_1$ ,  $q_2$ ,  $q_3$  and the parameters  $\gamma_1$ ,  $\gamma_2$ ,  $\gamma_3$  were chosen so that the stability condition in (23) is satisfied, while achieving a reasonable good performance according to the frequency response of the sensitivity function  $\zeta_o$ . The resulting sensitivity functions  $\zeta_o$ , for all the cases considered here, are shown in Fig. 7. Since the resulting repetitive controllers are LTI, with the use of a model of the open-loop system and the baseline controllers, stability robustness can be analyzed using the classical indices *minimum gain margin* (MGM) and *minimum phase margin* (MPM). This

TABLE I

EXPERIMENTAL RESULTS (BASELINE  $3\sigma = 4.9896$ ). INDEX  $3\sigma$  OBTAINED WITH THE ADAPTIVE-REPETITIVE SCHEME AT LOCATION {HEAD 1, TRACK 20,000}, FOR CASES: ONE-PERIOD (120 Hz), TWO-PERIOD (70 Hz, 120 Hz), THREE-PERIOD (70 Hz, 120 Hz, 407 Hz).

Algorithm / Order of $Q$	One-period	Two-period	Three-period
No Filter $Q$	4.4176	4.2805	3.9557
Inverse QR-RLS / 16	3.9218	4.0497	3.8292
Inverse QR-RLS / 64	3.7396	3.9122	3.6979
LMS / 16	4.1380	4.1275	3.9009
LMS / 64	4.0797	4.0791	3.8972
LMS / 128	3.9617	4.0454	3.8903
LMS / 256	3.9362	4.0157	3.8871

analysis was done and in all the cases  $MGM > 1.48$  dB and  $|MPM| > 29.5$  deg. The details are omitted for brevity.

### C. Experimental Results

The experimental effectiveness of the proposed control scheme is demonstrated using two sets of data. The first set of data was obtained at a specific location of the HDD (Head 1, Track 20,000), where several tests were performed in real-time. Those are summarized in Table I, Fig. 8 and Fig. 9. Fig. 8 compares the PSDs of the PES  $y$  for the cases: baseline control (blue), three-period repetitive control (green), and three-period adaptive-repetitive control using the inverse QR-RLS algorithm with a filter  $Q$  of order 64 (red). There, it can be observed that the LTI three-period repetitive controller is capable of canceling the periodic spikes at frequencies multiple of 70 Hz, 120 Hz and 407 Hz, while amplifying the inter-notch regions. This inter-notch amplification is canceled by the adaptive filter in the adaptive-repetitive scheme in Fig. 6. In order to clearly show the improvement in performance, Fig. 9 shows histograms comparing the PES  $y$  obtained with the use of the baseline controller and with the use of the adaptive-repetitive control scheme. Also using data obtained at location {Head 1, Track 20,000}, Table I compares the performances obtained using multiple-period repetitive controllers using various different parameters and in combination with the adaptive algorithms LMS and inverse QR-RLS.

The second set of data is summarized in Table II. There, we show the performance index value  $3\sigma$  for experiments performed at different locations of the HDD, employing the baseline controller, a LTI three-period repetitive controller (70 Hz, 120 Hz, 407 Hz), and the adaptive-repetitive scheme in Fig. 6, using the LMS and inverse QR-RLS algorithms with filters  $Q$  of orders 64 and 256, respectively. Clearly, the effectiveness of the proposed method is demonstrated.

## VI. CONCLUSIONS

In this paper we presented a method for synthesizing multiple-period repetitive controllers integrable to a minimum variance control scheme that combines repetitive and adaptive components. The main result presented here is a theorem that states a particular solution to the multiple-period repetitive control problem. The theorem was proved

TABLE II  
PERFORMANCE INDEX  $3\sigma$  OF THE *Position Error Signal (PES)* AS PERCENTAGE OF THE TRACK WIDTH.

	Head 0			Head 1		
	$y_{ref} = 10,000$	$y_{ref} = 15,000$	$y_{ref} = 20,000$	$y_{ref} = 10,000$	$y_{ref} = 15,000$	$y_{ref} = 20,000$
Baseline Controller	5.1126	5.0913	4.9632	5.1097	5.2278	4.9896
Three-period Repetitive Control	4.1795	3.9186	4.0489	4.0646	3.9709	3.9557
Adaptive-repetitive – Three-period (inv. QR-RLS / 64)	3.9814	3.7126	3.8097	3.7278	3.7546	3.6979
Adaptive-repetitive – Three-period (LMS / 256)	3.9349	3.8114	3.9066	3.8053	3.8530	3.8871

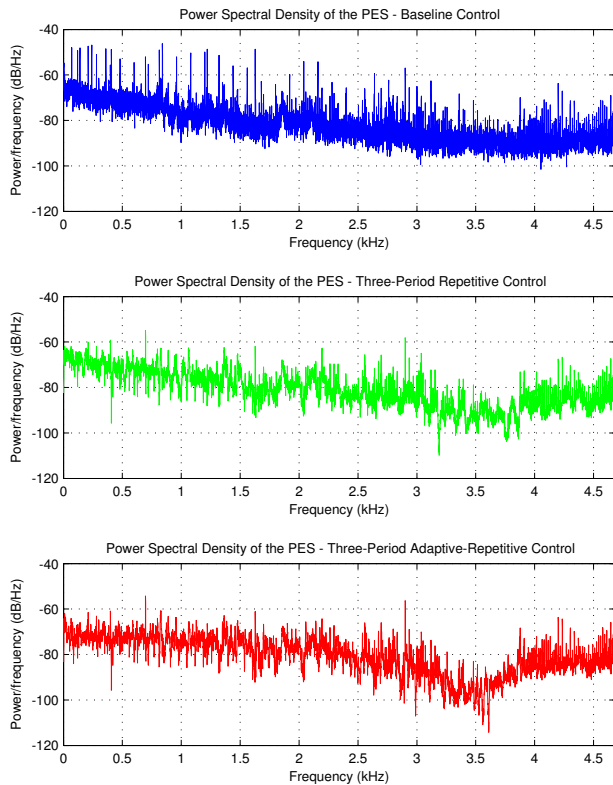


Fig. 8. Power spectral density of the PES  $y$  for three different experiments. *Upper Plot*: baseline Control. *Middle Plot*: three-period repetitive control (70 Hz, 120 Hz, 407 Hz). *Bottom Plot*: three-period adaptive-repetitive control.

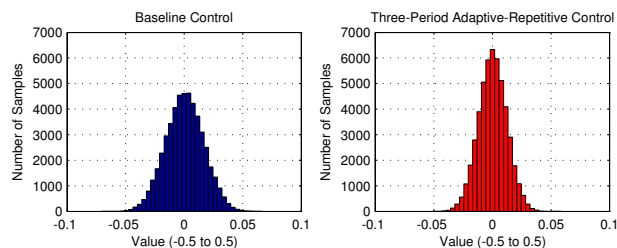


Fig. 9. Histogram comparing the experimental PES  $y$ , obtained with the use of the baseline controller and with the use of the multiple-period adaptive-repetitive control scheme (70 Hz, 120 Hz, 407 Hz).

using mathematical induction, and based on the proof, a method for synthesizing repetitive controllers recursively was derived. Experimental results, obtained using a hard disk drive, demonstrate the effectiveness of the proposed method.

## VII. ACKNOWLEDGMENTS

The authors are indebted to Western Digital for providing the hard disk drive and electronic interface board used in this research.

## REFERENCES

- [1] S. Hara, Y. Yamamoto, T. Omata, and M. Nakano, "Repetitive Control System: A New Type Servo System for Periodic Exogenous Signals," *IEEE Transactions on Automatic Control*, vol. 33, no. 7, pp. 659–668, July 1998.
- [2] M. Tomizuka, T.-C. Tsao, and K.-K. Chew, "Analysis and Synthesis of Discrete-Time Repetitive Controllers," *ASME Journal of Dynamic Systems, Measurement, and Control*, vol. 111, no. 3, pp. 353–358, Sept. 1989.
- [3] N. O. Pérez Arancibia, C.-Y. Lin, T.-C. Tsao, and J. S. Gibson, "Adaptive-Repetitive Control of a Hard Disk Drive," in *Proc. 46th IEEE Conf. on Decision and Control*, New Orleans, LA, Dec. 2007, pp. 4519–4524.
- [4] B. A. Francis and W. M. Wonham, "The internal model principle of control theory," *Automatica*, vol. 12, no. 5, pp. 457–465, Sept. 1976.
- [5] R. Horowitz, B. Li, and J. W. McCormick, "Wiener-filter-based Minimum Variance Self-tuning Regulation," *Automatica*, vol. 34, no. 5, pp. 531–544, May 1998.
- [6] M. Yamada, Z. Riadh, and Y. Funahashi, "Design of Robust Repetitive Control System for Multiple Periods," in *Proc. 39th IEEE Conf. on Decision and Control*, Sydney, Australia, Dec. 2000.
- [7] S. S. Garimella and K. Srinivasan, "Application of Repetitive Control to Eccentricity Compensation in Rolling," *ASME Journal of Dynamic Systems, Measurement, and Control*, vol. 118, no. 4, pp. 657–664, Dec. 1996.
- [8] D. H. Owens, L. M. Li, and S. P. Banks, "Multi-periodic repetitive control system: a Lyapunov stability analysis for MIMO systems," *International Journal of Control*, vol. 77, no. 5, pp. 504–515, Mar. 2004.
- [9] K. J. Åström and B. Wittenmark, *Computer Controlled Systems*. Englewood Cliffs, NJ: Prentice-Hall, 1984.
- [10] M. Tomizuka, "Zero Phase Error Tracking Algorithm for Digital Control," *ASME Journal of Dynamic Systems, Measurement, and Control*, vol. 111, no. 1, pp. 65–68, Mar. 1987.
- [11] T.-C. Tsao and M. Tomizuka, "Robust Adaptive and Repetitive Digital Tracking Control and Application to a Hydraulic Servo for Noncircular Machining," *ASME Journal of Dynamic Systems, Measurement, and Control*, vol. 116, no. 1, pp. 24–32, Mar. 1994.
- [12] G. Hillerström and J. Sternby, "Application of Repetitive Control to a Peristaltic Pump," *ASME Journal of Dynamic Systems, Measurement, and Control*, vol. 116, no. 4, pp. 786–789, Dec. 1994.
- [13] V. Kučera, *Discrete Linear Control*. Prague, Czechoslovakia: ACADEMIA, 1979.
- [14] M. A. Dahle and I. J. Diaz-Bobillo, *Control of Uncertain Systems*. Englewood Cliffs, NJ: Prentice Hall, 1995.
- [15] K. Zhou, J. C. Doyle, and K. Glover, *Robust and Optimal Control*. Upper Saddle River, NJ: Prentice Hall, 1996.
- [16] N. O. Pérez-Arancibia, T.-C. Tsao, and J. S. Gibson, "Saturation-Induced Instability and its Avoidance in Adaptive Control of Hard Disk Drives," *Accepted for publication in IEEE Transactions on Control Systems Technology*, available at <http://www.seas.ucla.edu/~nestor/publications.htm>.
- [17] A. H. Sayed, *Fundamentals of Adaptive Filtering*. New York, NY: Wiley, 2003.
- [18] N. O. Pérez Arancibia, T.-C. Tsao, and S. Gibson, "Adaptive Tuning and Control of a Hard Disk Drive," in *Proc. of the American Control Conference*, New York, NY, June 2007, pp. 1526–1531.